


[View Journal Online](#)
[View Article Online](#)

Synthesis, structure and hydrogen sorption properties of a pyrazine-bridged copper(I) nitrate metal-organic framework

 Emmanuel Ngwang Nfor ^{1,2,*}, Andrew David Burrows ², Bridget Ndoye Ndosiri ³,
 Luke Lawrence Keenan ⁴ and Offiong Efanga Offiong ⁵
¹ Department of Chemistry, Faculty of Science, University of Buea, Buea, Cameroon
nfor.emmanuel@ubuea.cm (E.N.N.)

² Department of Chemistry, University of Bath, Claverton Down, Bath BA2 7AY, United Kingdom
a.d.burrows@bath.ac.uk (A.D.B.)


³ Inorganic Chemistry Department, Faculty of Science, University of Yaounde 1, Yaounde, Cameroon
ndosirin@yahoo.com (B.N.N.)

⁴ Diamond Light Source, Didcot, Oxfordshire, OX11 0DE, United Kingdom
luke.keenan@diamond.ac.uk (L.L.K.)

⁵ Department of Pure and Applied Chemistry, University of Calabar, PMB 1115, Calabar, CRS, Nigeria
offiongeo@yahoo.com (O.E.O.)

* Corresponding author at: Department of Chemistry, Faculty of Science, University of Buea, Buea, Cameroon.
 Tel: +237.67.4519817 Fax: +237.33.322272 e-mail: nfor.emmanuel@ubuea.cm (E.N. Nfor).

RESEARCH ARTICLE


 10.5155/eurjchem.10.3.195-200.1888

 Received: 03 May 2019
 Received in revised form: 10 June 2019
 Accepted: 14 June 2019
 Published online: 30 September 2019
 Printed: 30 September 2019

KEYWORDS

 Copper
 Pyrazine
 Hydrogen sorption
 X-ray crystallography
 Single crystal structure
 Metal-organic framework

ABSTRACT

A new copper(I) pyrazine-bridged coordination polymer $[\text{Cu}_2(\text{pyz})_3(\text{NO}_3)_2] \cdot 2\text{DMF}$ (pyz = pyrazine) (1) has been synthesized and characterized by FT-IR, TG/DTG, DSC and single crystal X-ray diffraction techniques. The X-ray crystallographic result reveals a two-dimensional network structure containing hexagonal pores. Thermal analysis of compound 1 reveals it is stable to 380 °C, and gas sorption studies showed that it adsorbs 1.04 wt% hydrogen at 1 atm and 77 K. Compound 1 crystallizes in a triclinic system, space group *P*-1 (no. 2), $a = 7.9550(2)$ Å, $b = 7.9810(2)$ Å, $c = 11.0660(3)$ Å, $\alpha = 76.328(1)^\circ$, $\beta = 71.115(1)^\circ$, $\gamma = 84.577(1)^\circ$, $V = 645.79(3)$ Å³, $Z = 2$, $T = 150(2)$ K, $\mu(\text{MoK}\alpha) = 1.709$ mm⁻¹, $D_{\text{calc}} = 1.639$ g/cm³, 11111 reflections measured ($7^\circ \leq 2\theta \leq 54.96^\circ$), 2951 unique ($R_{\text{int}} = 0.0539$) which were used in all calculations. The final R_1 was 0.0346 ($>2\sigma(I)$) and wR_2 was 0.0727 (all data).

 Cite this: *Eur. J. Chem.* 2019, 10(3), 195-200

 Journal website: www.eurjchem.com

1. Introduction

The design and synthesis of metal-organic frameworks (MOFs) have received increasing attention due to their wide variety of fascinating topologies and potential applications in the fields of magnetism, catalysis, gas storage, conductivity, luminescence, non-linear optics [1-9] and drug delivery systems [10-12]. For many applications, optimal implementation requires: (a) large pore volumes (b) phase purity, and (c) retention of porosity upon removal of guest molecules [13].

The construction of MOFs is dependent on several factors, such as the choice of ligands and metal ions, as well as the solvent, temperature and the ratio of the ligands to metal ions used in the synthesis [9,14-16]. The most interesting versions of these materials display permanent nanoscale porosity, a feature that can translate into large internal surface areas,

ultralow densities, and the availability of uniformly structured cavities and portals of molecular dimensions. Importantly, the crystalline nature of MOF materials allows for unambiguous structure determination by X-ray diffraction methods. The resulting knowledge of atomic coordinates makes possible the application of high-quality computational modelling of static and dynamic interactions of MOFs with potential sorbents (i.e., predictive or explanative modelling of atomic and molecular isotherms, binding energies, and transport behaviour) [17-19]. Some of these properties are shared by other porous materials such as zeolites; however, MOFs diverge from zeolites in important ways. Perhaps the most significant difference lies in the element of chemical tunability embedded in the organic components of MOFs, which provides considerably greater structural diversity than is possible in zeolites [19]. Ligands with rigid backbones are often preferred in MOF synthesis

because, their rigidity makes it easier to predict the network geometry in advance of synthesis, and rearrangement to a denser phase on solvent removal is less favourable.

Among neutral ligands, pyrazines are especially useful as pillars in the construction of pillared-layer in 2D/3D network and pyrazine is a well-known bridging ligand that has been used in the preparation of MOFs [20,21]. Pyrazines have nitrogen lone electron pairs that are highly directional and have attracted much attention in the construction of supra-molecular structures such as porous materials [22,23] and molecular grids [24,25]. Herein, we report on the unanticipated reaction of pyrazine with copper(II) nitrate to form a copper(I) metal-organic framework.

2. Experimental

2.1. Materials and physical measurements

$\text{Cu}(\text{NO}_3)_2 \cdot 2.5\text{H}_2\text{O}$, pyrazine and the solvents were all used as purchased, without any further purification. The IR spectra were recorded on a Perkin-Elmer System 2000 FT-IR spectrometer scanning in the range of 4000-400 cm^{-1} using KBr pellets. The following indications are used to characterize absorption bands: very strong (vs), strong (s), medium (m), weak (w), shoulder (sh), and broad (br). Elemental analyses were performed on Perkin Elmer CHN-analyser. Thermogravimetric analysis (TGA) experiments were performed on a Shimadzu simultaneous TGA/DTG-60A compositional analysis instrument from room temperature to 800 °C in N_2 atmosphere at a heating rate of 5 °C/min and DSC analyses were recorded on a TA instrument, DSC-Q200, under dry nitrogen flow of 60 mL/min. Variable temperature PXRD analyses were conducted using the Bruker D8 Advance diffractometer equipped with a Lynx Eye detector using $\text{CuK}\alpha$ ($\lambda = 1.5406 \text{ \AA}$) at 298 K. The hydrogen adsorption measurements were performed using a Quantochrome iSorb-HP gas analyser at 77 and 87 K. Prior to the sorption experiments the sample of compound **1** was degassed by heating at 150 °C for 1.5 hours under dynamic vacuum.

2.2. Single crystal X-ray diffraction analysis and structure determination

The crystallographic data were collected on a Gemini diffractometer (Agilent Technologies) using $\text{MoK}\alpha$ radiation ($\lambda = 0.71073 \text{ \AA}$), ω -scan rotation. Data reduction was performed with the CrysAlis Pro [26] including the program SCALE3 ABSPACK [27] for empirical absorption correction. The structure was solved by direct methods (SHELXS-97 and SIR-92) and the refinement of all non-hydrogen atoms was performed with SHELXL-97 [28]. All non-hydrogen atoms were refined with anisotropic thermal parameters. For compound **1**, a difference-density Fourier map was used to locate all hydrogen atoms. The molecular graphics were done with ORTEP-3 [29] and Mercury (Version 3) [30].

2.3. Synthesis of the copper(I) MOF (1)

A mixture of $\text{Cu}(\text{NO}_3)_2 \cdot 2.5\text{H}_2\text{O}$ (0.696 g, 3 mmol) and pyrazine (0.240 g, 3 mmol), in 10 mL of DMF, 2 mL of ethanol was sealed in a 18 mL Teflon-lined autoclave and heated in an oven at 100 °C for 24 h. After slow cooling to room temperature, red acicular crystals of compound **1** were separated by filtration, washed repeatedly with DMF and soaked in anhydrous chloroform for 5 h. The resulting solid product was dried under vacuum at 120 °C for 4 h. Yield: 48%, based on Cu.

Anal. calcd. for $\text{C}_9\text{H}_{13}\text{CuN}_5\text{O}_4$: C, 33.88; H, 4.78; N, 21.95. Found: C, 34.20; H, 3.95; N, 22.52%. FT-IR (KBr, ν , cm^{-1}): 3458 (br), 3091 (m), 2932 (m), 2341 (m), 1657 (s), 1483 (s), 1427

(s), 1411 (s), 1304(s), 1093(s), 1038(s), 793(sh), 493(s), 417(s).

3. Results and discussion

The reaction between hydrated copper (II) nitrate and pyrazine in a 1:1 molar ratio in DMF:ethanol mixture at 100 °C for 24 hours, produced red acicular crystals in a 48% yield. The red colouration suggested the reduction of the Cu(II) metal centre to Cu(I) as corroborated by X-ray diffraction analysis. At high temperatures, nitrogen-rich organic ligands are well known to serve as effective reducing agents for such process [31].

3.1. Infrared spectra

The infrared spectrum of the uncoordinated pyrazine ligand exhibited a band at 417 cm^{-1} which shifted to higher frequency at 493 cm^{-1} in compound **1** upon coordination of the ligand to the metal centre [32]. The IR spectrum of compound **1** further exhibited strong vibrational bands at 1411, 1427 and 1488 cm^{-1} that were attributed to NO stretching vibrations for the monodentate nitrate group [33].

3.2. Crystal structure of compound 1

The structure of compound **1** with atomic numbering scheme is shown in Figure 1. The crystal structure refinement data of compound **1** is shown in Table 1, while selected bond lengths and bond angles are listed in Table 2.

The asymmetric unit of compound **1** consists of one Cu(I) centre, three independent pyrazine halves, each of which straddles a crystallographic inversion centre, one nitrate anion and one guest DMF molecule. The coordination geometry about each copper(I) ion is that of a distorted tetrahedron, with the coordination sphere containing three nitrogen atoms from pyrazine ligands and one oxygen atom from the nitrate ion. The Cu-N bond lengths involving the bridging pyrazine ligands are between 1.9721(17)-2.0445(18) Å. The oxygen atoms of the nitrate groups are considerably further from the copper(I) ion with a Cu-O bond length of 2.1660(16) Å. The Cu-N bond lengths within compound **1** are comparable to those observed for the equatorially bound pyrazine ligands in previously reported compounds [34-37], but shorter than those observed for the axially bound pyrazine ligands in $\text{Cu}(\text{pyz})_2(\text{CH}_3\text{SO}_3)_2$ (2.692(3) Å) [37] and $\text{Cu}(\text{pyz})(\text{hfac})_2$ (2.529(3) Å) [38]. The Cu...Cu separation across the bridging pyrazine group is 6.825 Å.

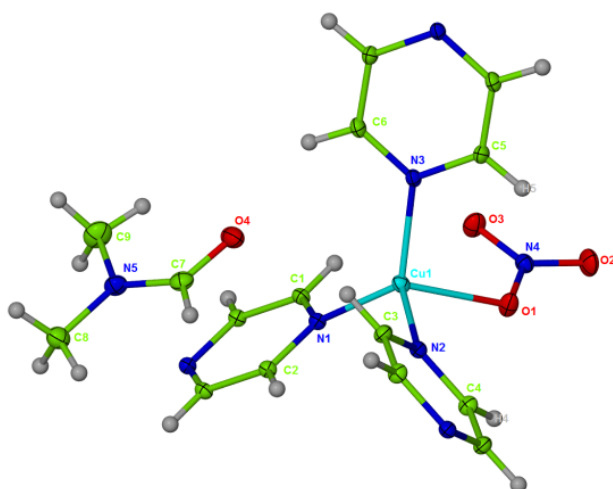
Overall, the pyrazine linkers connect the copper(I) centres into sheets with 6^3 topology, with each $\text{Cu}_6(\text{pyz})_6$ ring being in the chair conformation (Figure 2a). The sheets are packed in an offset manner so that channels are present along the crystallographic *b* axis (Figure 2b), and the included DMF molecules reside in these. Despite the ubiquity of pyrazine as a linker in MOF chemistry, the two-dimensional network structure observed in compound **1** is unusual, with only one previous report. The compound $[\text{Cu}_2(\text{pyz})_3(\text{ClO}_4)_2]$, prepared from the reaction of $\text{Cu}(\text{ClO}_4)_2 \cdot 6\text{H}_2\text{O}$ with pyrazine in the presence of 2,3-dihydroxyfumaric acid, forms a similar topology network to compound **1**, though the sheets are considerably more puckered [39]. Notably, when this reaction was carried out using $\text{Cu}(\text{NO}_3)_2 \cdot 2.5\text{H}_2\text{O}$ as the copper source, it yielded a different product to compound **1**, and the compound $[\text{Cu}(\text{pyz})(\text{NO}_3)]$ has a structure in which copper(I)-pyrazine chains are cross-linked into sheets by bridging nitrate ions [40]. The related ligands 2-methyl pyrazine and 2,3-dimethyl pyrazine form similar topology networks to compound **1** with copper(I), though in this case the pores are filled with polyoxometallate anions [41].

Table 1. Crystal data and details of the structure refinement for compound 1.

Parameters	Compound1
Empirical formula	C ₆ H ₁₃ CuN ₅ O ₄
Formula weight	318.78
Temperature (K)	150(2)
Crystal system	Triclinic
Space group	<i>P</i> -1
<i>a</i> (Å)	7.9550(2)
<i>b</i> (Å)	7.9810(2)
<i>c</i> (Å)	11.0660(3)
α (°)	76.328(1)
β (°)	71.115(1)
γ (°)	84.577(1)
Volume (Å ³)	645.79(3)
<i>Z</i>	2
ρ_{calc} (g/cm ³)	1.639
μ (mm ⁻¹)	1.709
<i>F</i> (000)	326
Crystal size (mm ³)	0.20 × 0.10 × 0.05
Radiation	MoK α (λ = 0.71073)
2 θ range for data collection (°)	3.50 to 27.48
Index ranges	-10 ≤ <i>h</i> ≤ 10, -10 ≤ <i>k</i> ≤ 10, -14 ≤ <i>l</i> ≤ 14
Reflections collected	11111
Independent reflections	2951 [<i>R</i> (int) = 0.0539]
Data/restraints/parameters	2951 / 0 / 174
Goodness-of-fit on <i>F</i> ²	1.054
Final <i>R</i> indexes [<i>I</i> ≥ 2 σ (<i>I</i>)]	<i>R</i> 1 = 0.0346 <i>wR</i> 2 = 0.0669
Final <i>R</i> indexes [all data]	<i>R</i> 1 = 0.0524 <i>wR</i> 2 = 0.0727
Largest diff. peak/hole (e.Å ⁻³)	0.316 and -0.649
Flack parameter	-0.6(10)

Table 2. Selected bond lengths [Å] and angles [°] for compound 1.

Bond lengths			
Cu(1)-N(1)	1.9720(17)	Cu(1)-N(3)	2.0108(17)
Cu(1)-N(2)	2.0443(18)	Cu(1)-O(1)	2.1660(16)
O(1)-N(4)	1.274(2)	O(2)-N(4)	1.237(2)
O(3)-N(4)	1.246(2)	O(4)-C(7)	1.227(3)
N(5)-C(8)	1.452(3)	C(1)-C(2)#1	1.380(3)
C(2)-C(1)#1	1.380(3)	C(3)-C(4)#2	1.382(3)
C(4)-C(3)#2	1.382(3)	C(5)-C(6)#3	1.380(3)
C(6)-C(5)#3	1.380(3)		
Bond angles			
N(1)-Cu(1)-N(3)	125.60(7)	N(1)-Cu(1)-N(2)	111.52(7)
N(3)-Cu(1)-N(2)	105.15(7)	N(1)-Cu(1)-O(1)	112.54(7)
N(3)-Cu(1)-O(1)	101.48(7)	N(2)-Cu(1)-O(1)	96.28(7)
N(4)-O(1)-Cu(1)	115.53(13)	C(1)-N(1)-C(2)	115.77(17)
O(2)-N(4)-O(3)	121.20(19)	O(2)-N(4)-O(1)	119.75(19)
O(3)-N(4)-O(1)	119.05(19)	C(7)-N(5)-C(9)	120.7(2)
N(1)-C(1)-C(2)#1	122.22(19)	N(1)-C(2)-C(1)#1	122.01(19)
N(2)-C(3)-C(4)#2	121.7(2)	N(2)-C(4)-C(3)#2	121.8(2)
N(3)-C(5)-C(6)#3	121.9(2)	N(3)-C(6)-C(5)#3	122.22(19)

Symmetry codes: #1 -*x* + 1, -*y* + 1, -*z* + 1, #2 -*x*, -*y* + 1, -*z* + 2, #3 -*x* + 1, -*y*, -*z* + 2.**Figure 1.** Asymmetric unit of compound 1 with atom numbering scheme at 50% probability level.

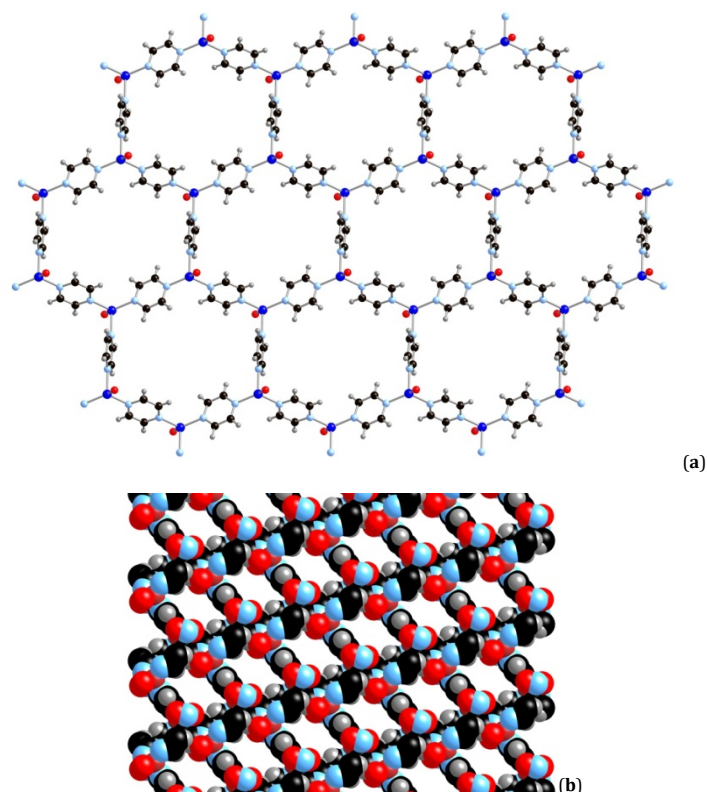


Figure 2. (a) View of the two-dimensional polymeric structure of compound **1**. DMF molecules in the pores have been omitted for clarity; (b) Space-filling representation of the structure of compound **1** showing the pores that are occupied by DMF molecules in the crystal structure. These molecules have been removed for clarity.

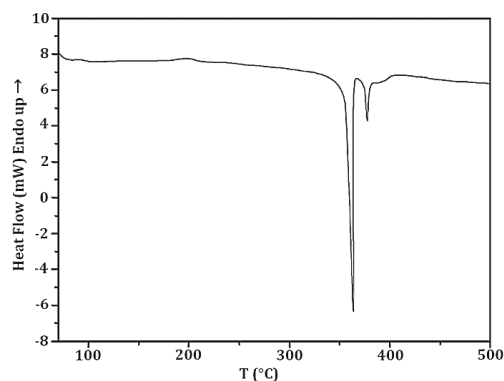


Figure 3. DSC curve of compound **1**.

3.3. Thermal behaviour of compound **1**

The thermal stability of compound **1** was analyzed by TG/DTG and DSC experiments as depicted in Figures 3 and 4, respectively. The DSC curve reveals a weak endothermic peak at approximately 200 °C and two exothermic peaks at 370 and 380 °C. The TGA results indicate that compound **1** is stable to 380 °C when decomposition of the framework starts. This is confirmed by the DTG curve with a characteristic intense exothermic peak at 370 °C followed by another weak exothermic peak at 392 °C. Overall the thermal analysis of the synthesized complex indicated an intense exothermic decomposition occurring between 350-400 °C.

3.4. Powder X-ray diffraction

The phase purity of compound **1** was confirmed by PXRD analysis, in which the experimental PXRD pattern was

consistent with the simulated PXRD pattern calculated from the single crystal data (Figure 5).

3.5. Activation

A three step activation process was carried out on the as-synthesized MOF **1** as follows. It was washed three times with DMF/DEF and the solvent exchange of DMF/DEF for CHCl_3 was carried out in which the samples was washed with lower boiling point solvent for removal of the first solvent from the pore.

For implementing this exchange, the mixture was immersed in CHCl_3 for 4 days and then the solvent removed under mild conditions after which the sample was filtered under vacuum at 120 °C for 8 hours [42].

The chemical stability of the thermally activated sample (0.05 g) of compound **1** was assessed by stirring it in ethanol under ambient condition for 5 hrs.

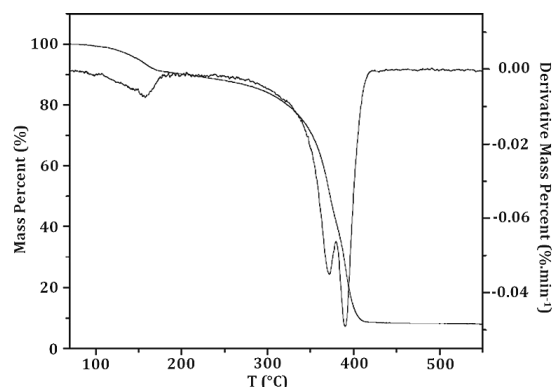


Figure 4. TG-DTG curve of compound 1.

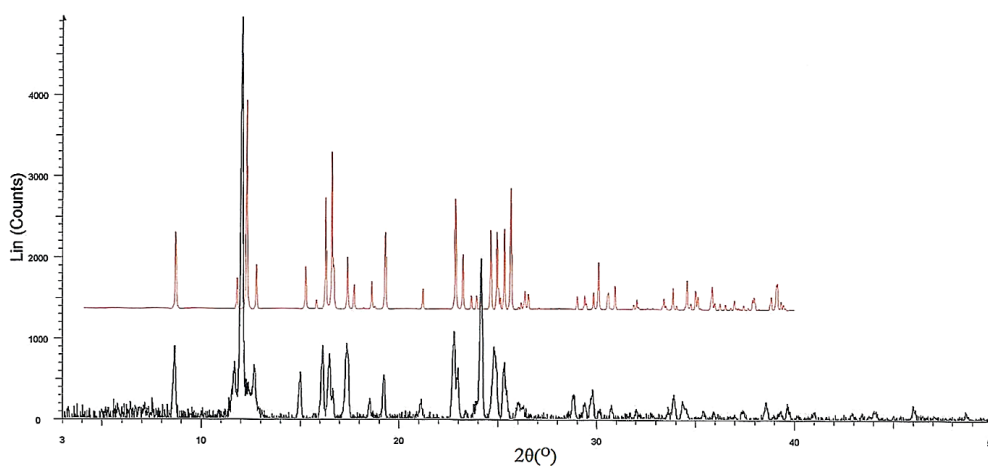


Figure 5. The experimental and simulated PXRD pattern of compound 1.

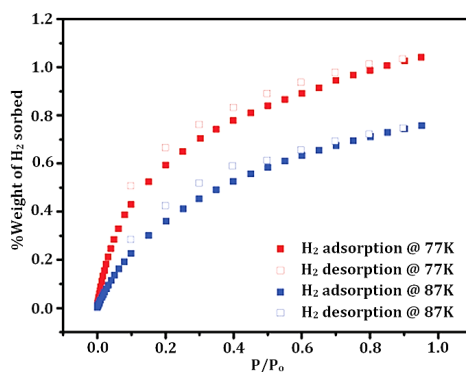


Figure 6. H₂ adsorption and desorption curves for compound 1 at 77 K (red) and 87 K (blue).

After collecting the samples by filtration, the crystallinity was examined by PXRD (Figure 5). Compound 1 retained its crystallinity following this treatment, confirmed by PXRD.

3.6. Gas adsorption properties of compound 1

Gas sorption experiments were performed in order to estimate the effect of the removal of DMF on the microporosity and on the accessible internal surface area of the metal-organic framework. To evaluate the porous properties of the framework, the desolvated solid of compound 1 was investigated for H₂ gas sorption measurements with the result suggesting reasonably porous properties and gas adsorption capability. The adsorption curve of compound 1, revealed a

type 1 isotherm, typical of microporous material [43]. The apparent BET surface areas for compound 1 of 512 m²/g and pore volume of 0.203 mL/g were determined based on the Ar adsorption isotherm at 77 K. The H₂ adsorption isotherms were carried out on compound 1 at both 77 and 87 K from 0 to 1.0 atm (Figure 6). The isotherm at 77 K displayed a maximum uptake of 1.04 wt% H₂ at 1.0 atm.

4. Conclusion

In conclusion, we report the synthesis and characterization, of a new copper(I) pyrazine-bridged coordination network structure. The material has been shown to be porous and able to absorb 1.04 wt% hydrogen gas at 77 K and 1 atm.

Acknowledgements

Emmanuel Ngwang Nfor is thankful to the Commonwealth Scholarship Commission (CSC) for Research Fellowship and Department of Chemistry, University of Bath, United Kingdom for hosting the fellowship

Supporting information

CCDC-1547134 contains the supplementary crystallographic data for this paper. These data can be obtained free of charge via <https://www.ccdc.cam.ac.uk/structures/>, or by e-mailing data_request@ccdc.cam.ac.uk, or by contacting The Cambridge Crystallographic Data Centre, 12 Union Road, Cambridge CB2 1EZ, UK; fax: +44(0)1223-336033.

Disclosure statement

Conflict of interests: The authors declare that they have no conflict of interest.


Author contributions: All authors contributed equally to this work.

Ethical approval: All ethical guidelines have been adhered.


Sample availability: Samples of the compounds are available from the author.

ORCID


Emmanuel Ngwang Nfor

 <http://orcid.org/0000-0003-4941-3917>


Andrew David Burrows

 <http://orcid.org/0000-0002-9268-4408>


Bridget Ndoye Ndosiri

 <http://orcid.org/0000-0001-7969-8963>

Luke Lawrence Keenan

 <http://orcid.org/0000-0001-9892-7864>

Offiong Efang Offiong

 <http://orcid.org/0000-0002-7784-4821>

References

- Batten, S. R.; Robson, R. *Angew. Chem. Int. Ed.* **1998**, *37*, 1460-1494.
- Eddaoudi, M.; Kim, J.; Rosi, N.; Vodak, D.; Wachter, J.; O'Keeffe, M.; Yaghi, O. M. *Science* **2002**, *295*, 469-472.
- Farrusseng, D.; Aguado, S.; Pinel, C. *Angew. Chem. Int. Ed.* **2009**, *48*, 7502-7513.
- Rowse, J. L. C.; Yaghi, O. M. *Angew. Chem. Int. Ed.* **2005**, *44*, 4670-4679.
- Leininger, S.; Olenyuk, B.; Stang, P. J. *Chem. Rev.* **2000**, *100*, 853-908.
- Cheng, X.; Liu, T.; Duan, X.; Wang, F.; Meng, Q.; Lu, C.; *Cryst. Eng. Comm.* **2011**, *13*, 1314-1321.
- Zang, S.; Su, Y.; Li, S.; Ni, Z.; Meng, Q. *Inorg. Chem.* **2006**, *45*(1), 174-180.
- Hasegawa, S.; Horike, S.; Matsuda, R.; Furukawa, S.; Mochizuki, K.; Kinoshita, Y.; Kitagawa, S. *J. Am. Chem. Soc.* **2007**, *129*, 2607-2614.
- Arici, M.; Yesilel, O. Z.; Keskin, S.; Tas, M. *Polyhedron* **2012**, *45*, 103-106.
- Horcajada, P.; Serre, C.; Vallet-Regi, M.; Sebba, M.; Taulelle, F.; Ferey, G. *Angew. Chem. Int. Ed.* **2006**, *118*, 6120-6124.
- An, J.; Geib, S. J.; Rosi, N. L. *J. Am. Chem. Soc.* **2009**, *131*, 8376-8377.
- Taylor-Pashow, K. M. L.; Rocca, J. D.; Xie, Z.; Tran, S.; Lin, W. *J. Am. Chem. Soc.* **2009**, *131*, 14261-14263.
- Sethi, N. K. PhD Thesis, Preparation of Heterobimetallic catalyst, York University, 2013.
- Wen, G. L.; Wang, Y. Y.; Zhang, W. H.; Ren, C.; Liu, R. T.; Shi, Q. Z. *Cryst. Eng. Comm.* **2010**, *12*, 1238-1251.
- Sun, D.; Luo, G. G.; Zhang, N.; Chen, J. H.; Huang, R. B.; Lin, L. R.; Zhang, L. S. *Polyhedron* **2009**, *28*, 2983-2988.
- Munakata, M.; Wu, L. P.; Kuroda-Sowa, T.; Maekawa, M.; Moriwaki, K.; Kitagawa, S. *Inorg. Chem.* **1997**, *36*(23), 5416-5418.
- Duren, T.; Bae, Y. S.; Snurr, R. Q. *Chem. Soc. Rev.* **2009**, *38*, 1237-1247.
- Han, S. S.; Mendoza-Cortes, J. L.; Goddard, W. A. *Chem. Soc. Rev.* **2009**, *38*, 1460-1476.
- Farha, O. K.; Hupp, J. T. *Accoun. Chem. Res.* **2010**, *43*(8), 1166-1175.
- Real, J. A.; Munno, G. D.; Munoz, M. C.; Julve, M. *Inorg. Chem.* **1991**, *30*, 2701-2704.
- Otieno, T.; Gipson, A. M.; Parkin, S. J. *Chem. Crystallogr.* **2002**, *2*(3-4), 81-85.
- Kitagawa, S.; Kitaura, R.; Noro, S. *Angew. Chem., Int. Ed.* **2004**, *43*(18), 2334-2375.
- Navarro, J. A. R.; Barea, E.; Galindo, M. A.; Salas, J. M.; Romero, M. A.; Quiros, M.; Masciocchi, N.; Galli, S.; Sironi, A.; Lippert, B. J. *Solid State Chem.* **2005**, *178*, 2436-2451.
- Ruben, M.; Rojo, J.; Romero-Salguero, F. J.; Uppadine, I. H.; Lehn, J. M. *Angew. Chem. Int. Ed.* **2004**, *43*(28), 3644-3662.
- Lehn, J. M. *Supramolecular Chemistry. Concept and Perspectives*, VCH, Weinheim, Germany, 1995.
- CrysAlis Pro: Data collection and data reduction software package, Agilent Technologies.
- SCALE3 ABSPACK: Empirical absorption correction using spherical harmonics.
- Sheldrick, G. M. *Acta Crystallogr. A* **2008**, *64*, 112-122.
- Farrugia, L. J. *J. Appl. Crystallogr.* **1997**, *30*, 565-565.
- Macrae, C. F.; Bruno, I. J.; Chisholm, J. A.; Edgington, P. R.; McCabe, P.; Pidcock, E.; Rodriguez-Monge, L.; Taylor, R.; Van de Streek, J.; Wood, P. A. *J. Appl. Crystallogr.* **2008**, *41*, 466-470.
- Otieno, T.; Rettig, S. J.; Thompson, R. C.; Trotter, B. *Can. J. Chem.* **1989**, *67*(11), 1964-1969.
- Nakamoto, K. *Infrared and Raman Spectra of Inorganic and Coordination Compounds*, Wiley-Interscience: New York, 1986.
- Lo, S. M. F.; Chu, S. S. Y.; Shek, L. Y.; Lin, Z.; Zhang, X. X.; Wen, G. H.; Williams, I. D. *J. Am. Chem. Soc.* **2000**, *122*, 6293-6294.
- Santoro, A.; Mighell, A. D.; Reimann, M. R. *Acta Crystallogr. B* **1970**, *26*, 979-984.
- Kuhlman, R.; Sehimek, G. L.; Kolis, J. W. *Polyhedron* **1999**, *18*, 1379-1389.
- Darriet, J.; Haddad, M. D.; Duesler, E. N.; Hendrickson, D. N. *Inorg. Chem.* **1979**, *18*(10), 2679-2682.
- Haynes, J. S.; Rettig, S. J.; Sams, J. R.; Thompson, R. C.; Trotter, J. *Can. J. Chem.* **1987**, *65*, 420-426.
- Belford, R. C. E.; Fenton, D. E.; Truter, M. R. *J. Chem. Soc. Dalton Trans.* **1974**, 17-24.
- The Cambridge Structural Database, Ref. code HUTW0J; Groom, C. R.; Bruno, I. J.; Lightfoot, M. P.; Ward, S. C. *Acta Crystallogr. B* **2016**, *72*, 171-179.
- Mohapatra, S.; Maji, T. K. *Dalton Trans.* **2010**, *39*, 3412-3419.
- Kong, X. J.; Ren, Y. P.; Zheng, P. Q.; Long, L. S.; Huang, R. B.; Zheng, L. S. *Inorg. Chem.* **2006**, *45*, 10702-10711.
- Aghajanoloo, M.; Rashidi, A. M.; Moosavian, M. A. *J. Chem. Eng. Process. Technol.* **2014**, *5*, 1-6.
- Hulvey, Z.; Sava, D. A.; Eckert, J.; Cheatham, A. K. *Inorg. Chem.* **2011**, *50*, 403-405.



Copyright © 2019 by Authors. This work is published and licensed by Atlanta Publishing House LLC, Atlanta, GA, USA. The full terms of this license are available at <http://www.eurjchem.com/index.php/eurjchem/pages/view/terms> and incorporate the Creative Commons Attribution-NonCommercial (CC BY NC) (International, v4.0) License (<http://creativecommons.org/licenses/by-nc/4.0>). By accessing the work, you hereby accept the Terms. This is an open access article distributed under the terms and conditions of the CC BY NC License, which permits unrestricted non-commercial use, distribution, and reproduction in any medium, provided the original work is properly cited without any further permission from Atlanta Publishing House LLC (European Journal of Chemistry). No use, distribution or reproduction is permitted which does not comply with these terms. Permissions for commercial use of this work beyond the scope of the License (<http://www.eurjchem.com/index.php/eurjchem/pages/view/terms>) are administered by Atlanta Publishing House LLC (European Journal of Chemistry).